Scalable stacked array piezoelectric deformable mirror for astronomy and laser processing applications

Wlodarczyk, Krystian; Bryce, Emma; Strachan, Mel; Hutson, David; Maier, Robert Raimund; Schwartz, Noah; Atkinson, David; Beard, Steven; Baillie, Tom; Parr-Burman, Phil; Kirk, Catherine; Hand, Duncan Paul

Published in:
Review of Scientific Instruments

DOI:
10.1063/1.4865125

Publication date:
2014

AIP | Review of Scientific Instruments

Scalable stacked array piezoelectric deformable mirror for astronomy and laser processing applications

Krystian L. Wlodarczyk, Emma Bryce, Noah Schwartz, Mel Strachan, David Hutson, Robert R. J. Maier, David Atkinson, Steven Beard, Tom Baillie, Phil Parr-Burman, Katherine Kirk, and Duncan P. Hand

Citation: Review of Scientific Instruments **85**, 024502 (2014); doi: 10.1063/1.4865125
View online: http://dx.doi.org/10.1063/1.4865125
View Table of Contents: http://scitation.aip.org/content/aip/journal/rsi/85/2?ver=pdfcov
Published by the AIP Publishing

Scalable stacked array piezoelectric deformable mirror for astronomy and laser processing applications

Krystian L. Wlodarczyk,[1,a)] Emma Bryce,[2] Noah Schwartz,[3] Mel Strachan,[1,3] David Hutson,[2] Robert R. J. Maier,[1] David Atkinson,[3] Steven Beard,[3] Tom Baillie,[3] Phil Parr-Burman,[3] Katherine Kirk,[2] and Duncan P. Hand[1]

[1]*Institute of Photonics and Quantum Sciences, Heriot-Watt University, Edinburgh EH14 4AS, United Kingdom*
[2]*School of Engineering and Science, University of the West of Scotland, Paisley PA1 2BE, United Kingdom*
[3]*UK Astronomy Technology Centre, Royal Observatory, Edinburgh EH9 3HJ, United Kingdom*

(Received 9 October 2013; accepted 27 January 2014; published online 12 February 2014)

A prototype of a scalable and potentially low-cost stacked array piezoelectric deformable mirror (SA-PDM) with 35 active elements is presented in this paper. This prototype is characterized by a 2 μm maximum actuator stroke, a 1.4 μm mirror sag (measured for a 14 mm $\times$ 14 mm area of the unpowered SA-PDM), and a $\pm$200 nm hysteresis error. The initial proof of concept experiments described here show that this mirror can be successfully used for shaping a high power laser beam in order to improve laser machining performance. Various beam shapes have been obtained with the SA-PDM and examples of laser machining with the shaped beams are presented. [http://dx.doi.org/10.1063/1.4865125]

I. INTRODUCTION

Recent developments in industrial lasers provide high quality, highly focused beams with a Gaussian intensity profile and a M^2 value that is close to the Gaussian diffraction limit ($M^2 \approx 1.1$). In some cases, however, the Gaussian intensity profile is not ideal for an intended task or process, and therefore it is necessary to reshape the spatial intensity distribution of the beam. For instance, flat top beams are more suitable for laser polishing,[1] donut-shaped beams with sharply defined edges are more efficient for laser drilling,[2] whilst elliptically shaped beams are known to be more beneficial for cutting,[3] dicing,[4] and also melting applications.[5] Creating an elliptically shaped beam along the scan direction can increase the cutting speed, improve the ablation efficiency, modify the laser-induced thermal gradient and stresses in the workpiece, and enhance the surface quality of laser-molten structures. Other, more complex intensity distributions might also be useful for surface micro-texturing applications.

The intensity distribution of laser beam can be changed by using passive optical components and active optical devices (i.e., wavefront correctors used in Adaptive Optics (AO) systems). The use of passive optical components, such as lenses, mirrors, and diffractive-optical elements (DOEs), enables a huge variety of laser beam profiles to be generated. However, every time a different beam shape is desired, a new (often bespoke) optic is required. In addition, any changes in the input beam profile would typically require the optics to be changed. This means that flexible shaping of the laser beam with passive optical components can be complicated and expensive. Instead, active optical devices, e.g., deformable mirrors (DMs), are used so that the laser beam intensity profile can be dynamically altered. This means that the beam shape can be altered "on-the-fly," and therefore it can be changed, e.g., between laser pulses during a laser machining process.

Originally, DMs were developed and applied for military and astronomy, e.g., in telescopes to correct wavefronts distorted by the earth's atmosphere in order to obtain an undistorted image of stars and galaxies.[6,7] Later, these devices became more available and started to be used in research, industry, and medicine.[8] Nowadays, DMs are also used to correct low-order aberrations, such as distortions caused by an optical system, and to modify the shape of an output laser beam.

There are a number of different types of DMs that can be used for wavefront modification. Based on the internal construction and operating principle, they can be broadly divided into three groups:[9] membrane deformable mirrors (MDMs), stacked array piezoelectric deformable mirrors (SA-PDMs), and bimorph mirrors (BMs). MDMs consist of a very thin high-reflecting (HR) coated membrane whose shape is controlled by electromagnetic forces induced between the membrane and a two-dimensional array of voice coils which are mounted to a base plate underneath the membrane. Although MDMs are generally characterized by large stroke capability and near zero hysteresis, they are relatively fragile and can pick up acoustic signals, which is a problem in noisy environments such as those typically found in laser machining.

SA-PDMs consist of a thin HR-coated continuous optical plate (generally fused silica, BK7, or silicon) which is bonded to a two-dimensional array of piezoelectric actuators, as can be seen in Fig. 1. In this type of deformable mirror, the optical plate is deformed when a voltage is provided to individual actuators, leading to their elongation or contraction. In commercially available SA-PDMs, the maximum actuator stroke can be up to approximately 10 μm whilst the inter-actuator stroke does not generally exceed 3 μm.[9,10] In contrast to

[a)]Author to whom correspondence should be addressed. Electronic mail: K.L.Wlodarczyk@hw.ac.uk

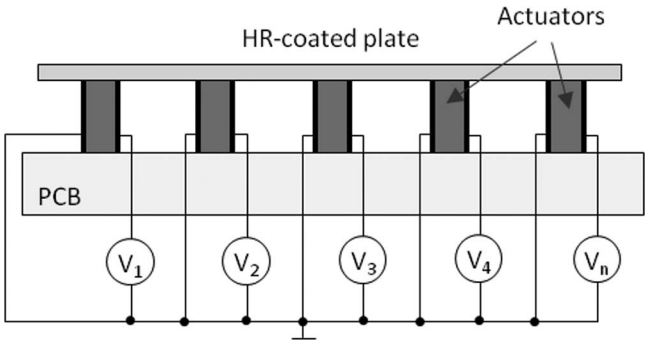

FIG. 1. Construction of stacked array piezoelectric deformable mirrors (SA-PDMs).

MDMs, SA-PDMs exhibit an inherent hysteresis between 5% and 15%, and therefore in practice these devices typically require a feedback loop for correct operation. These devices still tend to be very expensive, especially those with a large number of active elements. However, because of their robust construction, fast response rate (up to several kHz), high actuator count, and high laser power handling capabilities,[11] they are well suited for laser beam shaping applications.

The last group of DMs are BMs. These devices consist of a reflective surface bonded onto a two-layer piezoceramic, with metal electrodes located between the layers. Since the upper layer has an opposite polarization direction to the bottom layer, a voltage applied to one of the electrodes causes an in-plane expansion of one layer and an in-plane contraction of the other layer, thereby bending the piezoceramic and deforming the mirror that is laterally confined by the mount. Due to high laser power handling capabilities and relatively small sizes, BMs are well suited for laser beam shaping and can work in an intracavity arrangement to enhance the far-field brightness of solid-state lasers.[12] However, they generally have less than a couple of hundred actuators and have low resonant frequencies,[10] which make them less versatile (in terms of beam shaping capabilities) than SA-PDMs and MDMs.

An interesting group of active optical devices are spatial light modulators (SLM) based on liquid crystal displays. These electronically programmable devices provide the ability to modify both phase and amplitude of linearly polarized light. Although SLMs are characterized by very high spatial resolution (typically more than a half million pixels), which permits the generation of complex laser beam shapes and patterns, they are slower than DMs (frame rate $<$ 200 fps) and cannot handle such a high average laser power – typically 2 W/cm^2 and up to 10 W/cm^2 when a heat sink is mounted to the LC display.[13] Moreover, SLMs used as DOEs produce unwanted speckles that affect the quality of the image generated by the SLM display. Although the speckles can be reduced by the "time-averaging" technique,[14,15] they cannot be completely removed due to the pixilated (digital) character of the LC display that introduces the discontinuity to the computer-generated hologram.

Digital micro-mirror devices (DMDs)[16–19] represent a further beam shaping technology, which like SLMs, have been originally developed for image projection.[15] DMDs are very fast devices (frame rate $>$ 20 000 fps) and consist of a large number of micro-mirrors (e.g., 1024 $\times$ 768 elements). In comparison to SLMs, DMDs exhibit a slightly higher diffraction efficiency (approximately 65%[19] compared to 55% in SLMs[20]) and laser damage threshold of 12 W/cm^2. Recently, DMDs have been successfully used in the multi-photon lithography[21] and the laser-induced forward transfer (LIFT) process.[22,23] Micro-Electro-Mechanical Systems (MEMS) deformable mirrors are a similar alternative technology to DMDs. However, their main drawback is that they are not well suited for laser applications because of their low power handling capabilities and their very small size.[24,25]

Among the large variety of active optical devices described above, the SA-PDMs appear best suited to laser processing. Good laser power handling capabilities combined with a high speed and mechanical robustness of SA-PDMs means that these devices can easily work with many industrial lasers.

This paper describes a laboratory demonstrator of potentially low-cost and scalable SA-PDM, called "36DM1," which was developed by the University of the West of Scotland (UWS) and the United Kingdom Astronomy Technology Centre (UK-ATC). The performance, key features, and application of the 36DM1 device for laser material processing are presented in this work. The mirror described here contains 35 actuators, and therefore has a similar number of active elements as a commercially available 37-element PDM from OKO Technologies.[11] In contrast to the OKO PDM, our mirror has a smaller aperture and a different shape, i.e., it is a 20 mm square plate rather than a 30 mm diameter disk, and the actuators are arranged in a 6 $\times$ 6 array rather than in a hexagonal pattern. This square array is used to match typical wavefront sensor geometry use in astronomy and to simplify the manufacturing process, whereby a diamond saw defines the actuators – see Sec. II below – which is a very important aspect in terms of the device scalability. This approach has significant promise for application in next-generation telescopes and instrumentation, e.g., the European Extremely Large Telescope (E-ELT).[26] In particular, we believe that the fabrication process of the device can be automated in the future; thereby piezoelectric deformable mirrors will be affordable for many researchers and industry.

II. 36DM1 DEVICE

Figure 2 shows the manufacture process of the 36DM1 device. An actuator array, which is mounted to a printed circuit board (PCB), was constructed from multilayer piezoceramic planks that were precision sawn to form the matrix of actuators. The actuator planks were layered with electrodes oriented lengthwise and in rows, as shown in Fig. 2(a). Afterwards, the top surface of the array was polished flat and the electrodes were precisely sawn in order to leave only a thin metallic layer from both sides of the planks, as can be seen in Fig. 2(b). The bottom of electrodes was soldered to the PCB tracking layer. In the next steps, the array was sawn across to create the square-based actuator pillars – see Fig. 2(c) – and the mirror was bonded onto the actuator array – see Fig. 2(d). More details can be found in our earlier publication.[27]

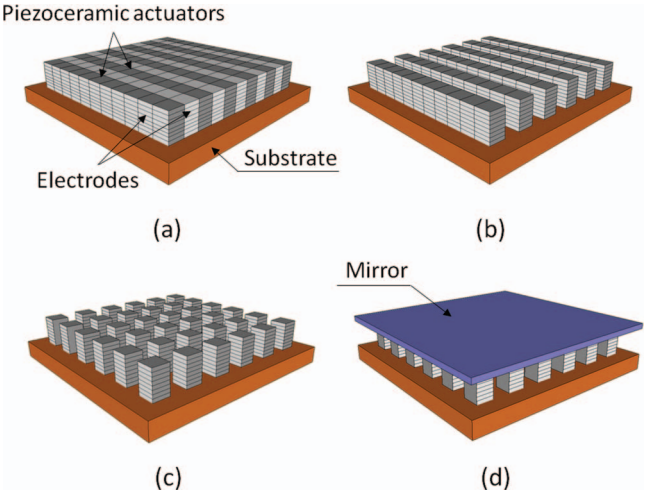

FIG. 2. (a)–(d) Piezoelectric deformable mirror fabrication.

The 36DM1 mirror was designed with actuators arranged in a 6 × 6 array. During the manufacturing process, one of the corner actuators was removed (after being damaged) and the device had 35 working elements.

The mirror substrate used was a 100 μm thick silicon plate which was coated with a dielectric designed to be highly reflective at a wavelength of 1064 nm. The reflectivity of the mirror was measured to be approximately 98% at the laser light incident angle of 5°, enabling (in theory) the mirror to be illuminated by a 50 W average power laser beam without damaging the silicon substrate. In our laboratory, we performed a laser-induced damage test for the HR-coated substrate using a 65 ns pulsed Yb:YVO4 laser (Spectra Physics Lasers, Inc.). During the test, it was found that the mirror can easily handle the average laser power density of 10 kW/cm^2.

The assembled 36DM1 device is shown in Fig. 3. The mirror is controlled by a commercially available high-voltage amplifier and USB DAC-40 unit from OKO Technologies. The control interface was created in the Graphical User Interface (GUI) of Matlab.

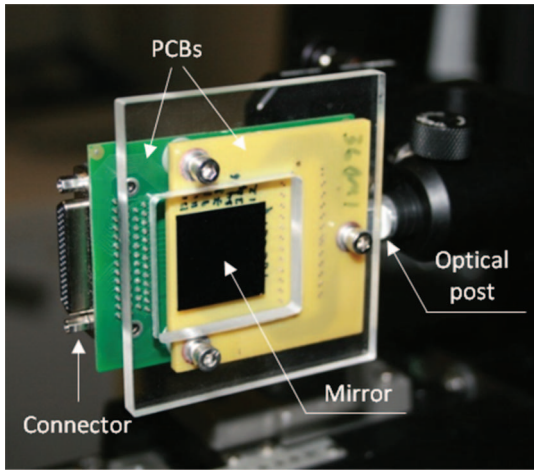

FIG. 3. Photograph of the 36DM1 device.

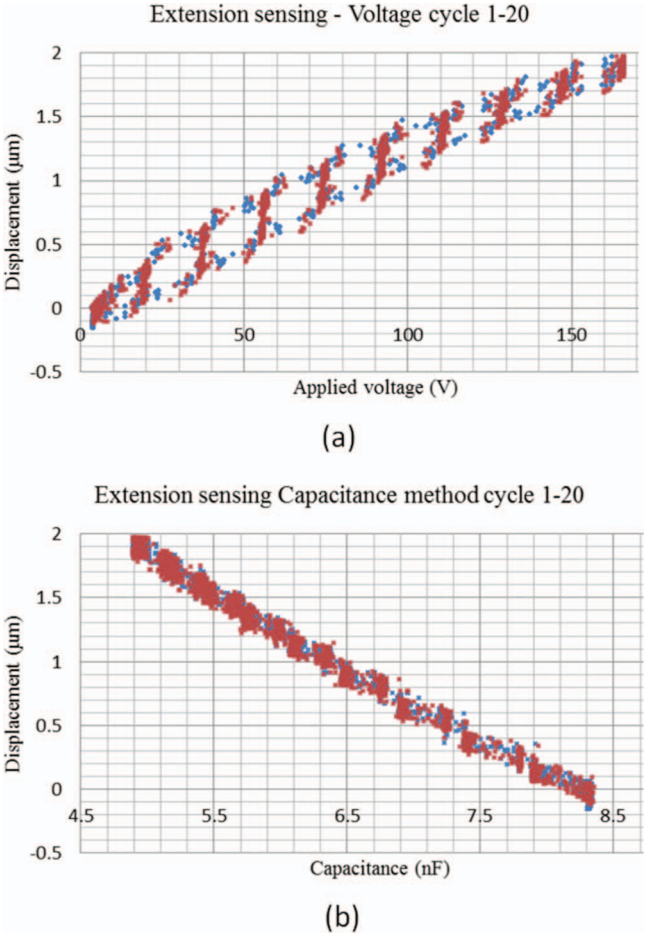

FIG. 4. Hysteresis in extension of a multilayered piezoelectric actuator over 20 full stroke voltage cycles measured by a MTI-2100 Fotonic fiber optic probe for: (a) displacement vs applied voltage and (b) displacement vs actuator capacitance at 20 kHz.

The maximum actuator stroke was measured to be 2 μm at the applied voltage of 170 V, as shown in Fig. 4(a). Measurements of the displacement of the top of the actuator under voltage drive were made using a MTI-2100 Fotonic fiber optic probe. The actuator extension increases with increasing applied voltage; however, we have observed a ± 200 nm hysteresis error. This means that over a full voltage cycle (0–170 V) the actuator extension can be up to 400 nm larger on the downward part of the cycle than on the upward part, for the same value of the applied voltage.

In order to reduce the hysteresis error, we can apply one of the extension sensing techniques reported by us,[28,29] which is based on capacitance measurement of actuators at 20 kHz. Using this technique the hysteresis error can be reduced to ± 75 nm, as can be seen in Fig. 4(b). Although the extension sensing based on capacitance measurement has not been used in the 36DM1 device for this work, this technique will be applied in the next version of SA-PDM, which is currently under development. The extension sensing method requires no further connections to each actuator, so it can also be applied to the existing mirror without additional wiring.

A non-contact 3D surface profilometer (Zygo) was used to determine shape of the unpowered deformable mirror. For

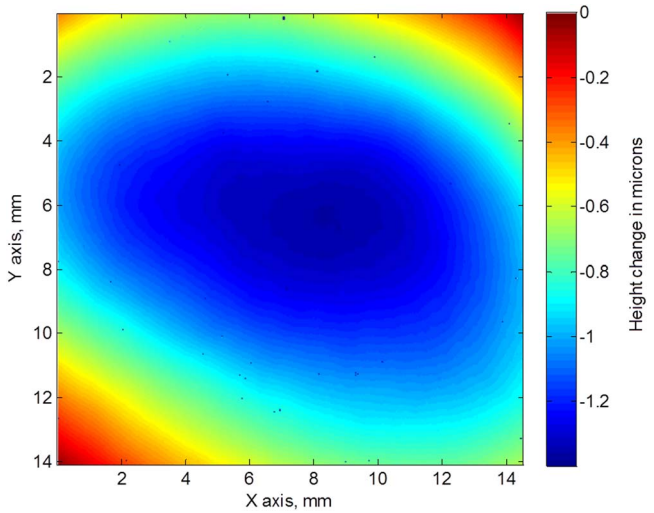

FIG. 5. Surface profiles of the unpowered 36DM1 mirror.

the mirror lying horizontally, it was found to have a concave shape with a sag of 0.45 μm across a 14.5 $\times$ 14.2 mm mirror area and a sag of 1.4 μm when measurement was taken along the one of its diagonals (see Fig. 5). Further investigation of the mirror shape has shown that the sag results from stresses in the dielectric coating and most likely it can be reduced by optimizing the stress properties in the HR coating. Since the mirror sag is within the range of the actuator extension, the SA-PDM can be flattened when actuated.

When the 36DM1 device was placed vertically, as shown in Fig. 3, and a 49-wire cable was plugged in to the connector, it was observed that the shape of mirror surface changed. Using the phase stepping interferometry – described elsewhere[13] – it was found that the mirror substrate acquires a kind of saddle shape, as shown in Fig. 6. Fortunately, the mirror sag still remains in the range of approximately 1.4 μm for a 14 $\times$ 14 mm mirror area and thus the mirror can be effectively flattened when actuated.

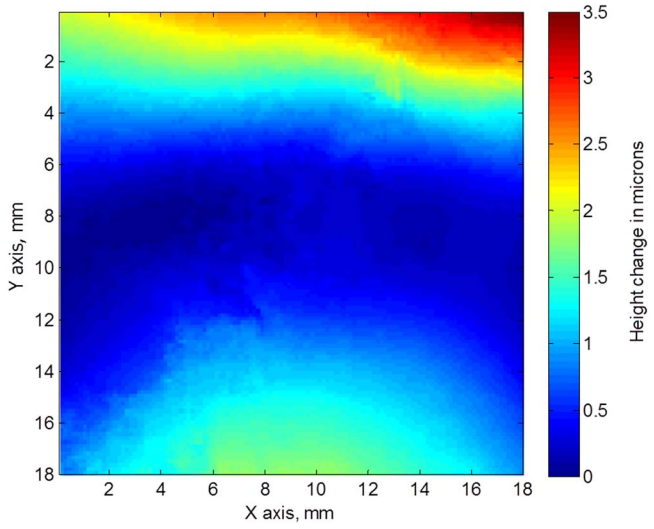

FIG. 6. 3D surface profile of the unpowered mirror when placed vertically in an optical holder. The profile was measured using a phase stepping interferometer.

It was found that the unwanted deformation of the mirror results from stresses induced by the connected cable and an optical post to which the PCB substrates were mounted (see Fig. 3). To solve this problem, we are planning to design a stress-free mount for the next version of SA-PDM which is currently under development. In the construction of the next generation mirror, we will attach the 49-way connector to a rigid metallic enclosure and ensure that the signals coming from the connector are delivered to the PCB via thin and flexible cables.

III. USE OF THE 36DM1 DEVICE FOR LASER MATERIALS PROCESSING

SA-PDMs are not readily used for laser processing because these optical devices are still very expensive, and their price can be even higher than the price of the lasers used for machining. However, our SA-PDM design should allow much cheaper fabrication, resulting in low cost DMs that will then be exploited across a wide range of applications. We therefore demonstrate the capability of the 36DM1 device for shaping a high power laser beam and apply this for processing a metal workpiece.

For this purpose, we used a Q-switched Nd:YVO_4 laser (Spectra Physics Lasers, Inc.) that provides 65 ns pulses with an average optical power of up 35 W at a wavelength of 1064 nm. The maximum pulse energy was 2.33 mJ. The output laser beam with a M^2 value of 1.3 was expanded by a $\times$5 magnification Galilean telescope, as shown in Fig. 7, giving a beam of approximately 12 mm diameter on the SA-PDM surface. The expanded beam was delivered at an incident angle of 5°. The beam reflected from the deformable mirror was subsequently reduced to a 4.5 mm diameter beam in order to match an input aperture of a galvo-scanner. The galvo-scanner was equipped with a 125.4 mm FL flat-field lens. Using a reference flat mirror instead of the 36DM1 device, the beam diameter in the focal plane of the F-theta lens was approximately 50 μm (measured at $1/e^2$ of its maximum intensity). The lenses f_3, f_4, and F-theta were in a 6-f optical arrangement.

Using a flip mirror and two lenses (f_5 = 75 mm and f_6 = 400 mm), the laser beam can be focused onto a

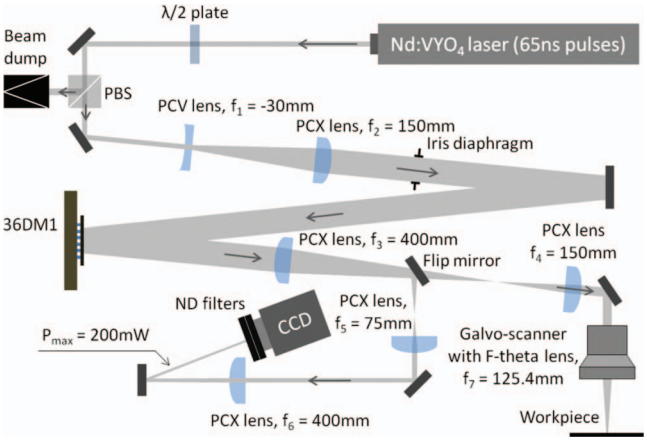

FIG. 7. Optical setup used to shape the laser beam with the 36DM1 device.

monochrome CCD camera for the closed-loop beam shaping. The lenses (f_5 and f_6) together with the lens f_3 are in a 6-f optical arrangement, so that the beam profile captured by the CCD camera has the same intensity distribution, but a different size, as the laser beam at the focal plane of the F-theta lens. The lens f_6 was chosen to have a long focal length of 400 mm to ensure that a sufficiently large laser spot is created on the CCD array. To prevent the CCD from saturation and laser-induced damage, two neutral density filters were mounted to the front of the camera.

Shaping the laser beam by the 36DM1 device was executed by the simulated annealing (SA) algorithm,[30] which was part of the closed-loop feedback between the beam profile captured by the CCD camera and the set of voltages written to the 36DM1 mirror actuators. We chose the SA algorithm because it had been already used with a good result with another deformable mirror, a 37-element PDM from OKO Technologies, to control the laser beam wavefront.[2,31,32] The advantage of the SA algorithm is that it enables the optimization of many variables simultaneously, i.e., the voltages of all actuators in the DM.

The SA algorithm is a stochastic method that enables the global minimum (or maximum) of some error function to be found. In our case, the error function was the root mean square (rms) of the difference between the spatial intensity beam profile of the target and the actual beam generated by the deformable mirror. Small vibrations of the laser beam focused on the CCD array, which resulted from the limited pointing stability of the laser (amplified by comparatively long optical path length) and vibrations coming from the external devices (e.g., a laser cooling system), were compensated by applying the centre of mass technique in the SA algorithm.

In order to run the SA algorithm, it is necessary to define three input parameters – the *change factor* (CF), the *algorithm temperature* (AT), and the number of iterations (N) – as well as the initial voltages of actuators and the image of the target beam profile that needs to be achieved on the CCD array. The *change factor* defines the magnitude of the random changes to generate a new set of actuator voltages, based on the current or initial set of actuator voltages. This factor needs to be selected very carefully because if the random changes are too small the algorithm can be trapped in a local minimum solution and will not be able to escape due to a too small step size. On the other hand, if the change factor is too high, the SA algorithm turns into a random search which is unable to zoom in to any minima solutions. The *algorithm temperature* is a parameter which is used to perform the Boltzmann probability test in the SA algorithm. Apart from the *algorithm temperature*, the probability test takes into account the rms error of the current beam and the rms error from the iteration that gave us the best result. Depending on the probability test result, a new set of actuator voltages is accepted or not for the next iteration. More details about the SA algorithm and its input parameters can be found elsewhere.[32]

Choosing appropriate starting conditions for the actuator voltages can significantly reduce the required number of iterations of the SA algorithm for the beam shape optimization, and hence reduce the time required to get the desired beam shape. In our proof of the concept experiment, however, this issue was not very important and thus the initial value of voltages was chosen to be identical (90 V) for all actuators, so the initial beam profile before the SA optimization was distorted – see Fig. 8. This resulted from the intrinsic curvature of the 36DM1 mirror, as discussed in Sec. II. The average speed of the SA algorithm used in our experiment was approximately 140 iterations per minute.

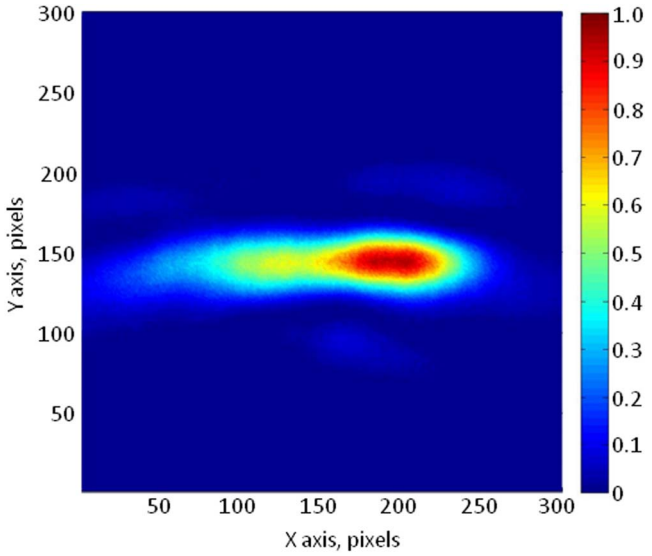

FIG. 8. Beam profile captured by the CCD camera when 90 V is written to all actuators in the 36DM1 mirror.

The proof of concept experiment was performed in order to demonstrate the beam shaping capability of the 36DM1 device. The aim of this experiment was to obtain different shapes of the laser beam on the CCD array and use these beam shapes for machining an aluminum workpiece. The laser machining was carried out at an average laser power of 15.8 W, pulse repetition frequency of 15 kHz, and pulse energy of 1.05 mJ.

In order to generate a desired beam shape with the use of the SA algorithm, the average laser power delivered to the CCD camera was reduced to approximately 200 mW, as indicated in Fig. 7, by rotating the $\lambda/2$ plate so that majority of the output laser power was redirected to the beam dump through the polarizing beam splitter (PBS). The beam shape optimization was carried out for different values of the input parameters (CF, AT, and N). In general, we managed to obtain different beam intensity profiles which were quite similar to the target designs. Some selected results are presented in Fig. 9.

The left column shows the target beams, whereas the middle column shows the best shaped beams including the values of the input parameters. In order to demonstrate the effect of SA-PDM-shaped beam on laser machining, the flip mirror was removed from the optical setup – see Fig. 7 – allowing the shaped beam to be delivered to the workpiece via the galvo-scanner. Machining of the aluminum plate was carried out at the average laser power of 15.8 W. This required the $\lambda/2$ plate to be rotated back to the initial position. The laser machining results are presented in the right column of Fig. 9. Each crater was generated by a single laser pulse, using the

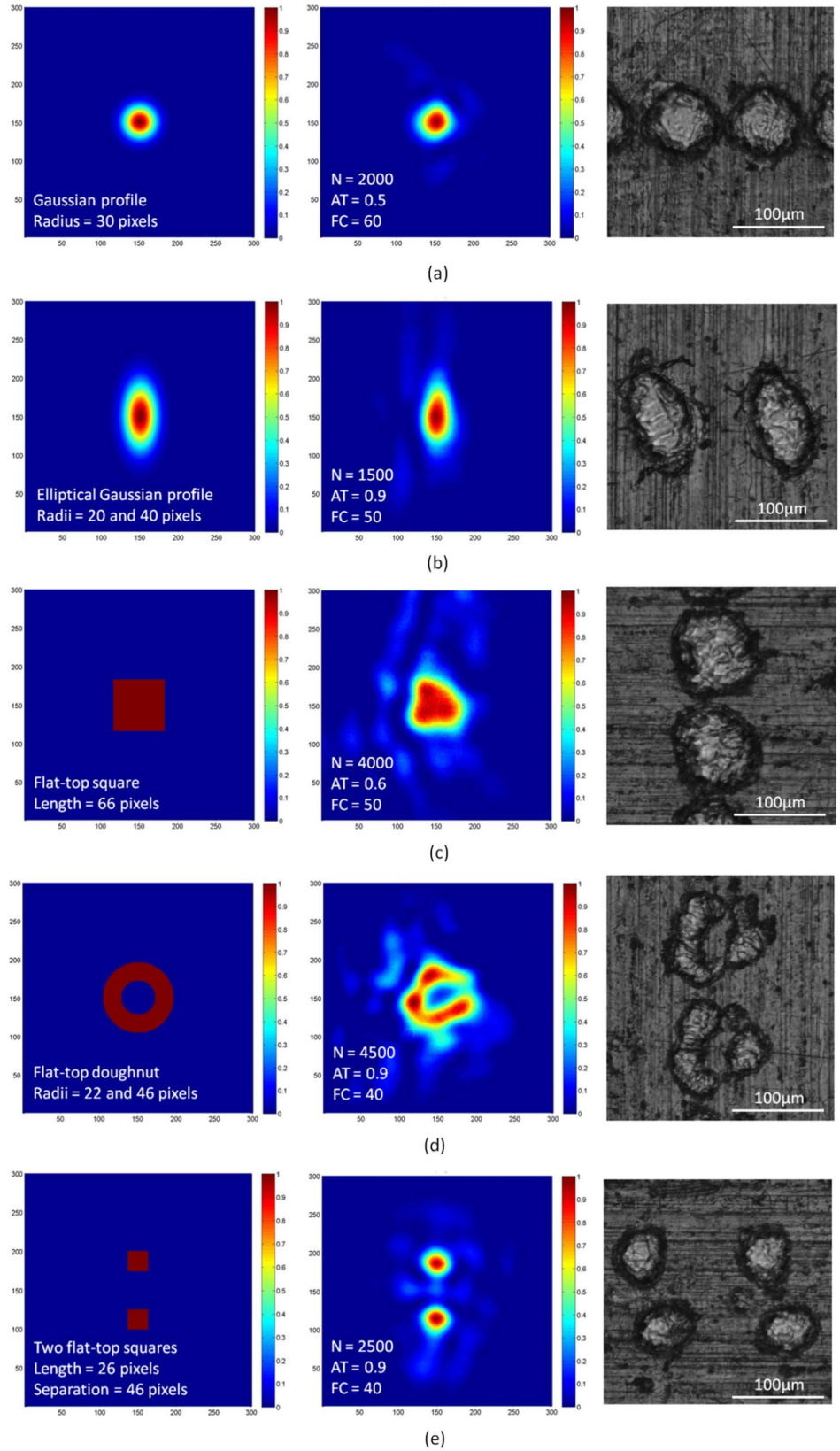

FIG. 9. (a)–(e) Different beams obtained with the 36DM1 mirror. Left column: target images; middle column: the best beam shaping results; right column: aluminium machined with the shaped laser beam.

SA-PDM-shaped beam that was moved with the speed of 2 m/s. This provided a 133 μm separation distance between the individual craters. All craters shown in Fig. 9 are skewed and this probably results from some small optics misalignment. Nevertheless, the results show clearly that the 36DM1 device can controllably generate various beam profiles for applications in different laser-based machining processes (e.g., laser marking, texturing, drilling, etc.).

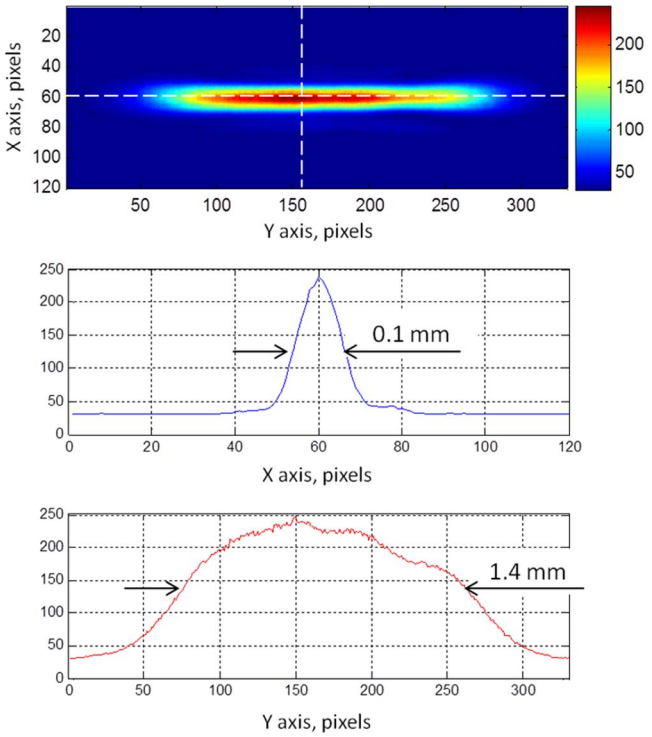

FIG. 10. Gaussian-distributed stripe generated by the reference flat mirror. Cross-section of the beam was taken along the dashed lines.

An interesting beam shape that can be obtained with a deformable mirror is a flat-top stripe, which can be used for the generation of sinusoidal gratings on metals, i.e., like those obtained by the *YAGboss* process.[5] Although the stripe can be produced by a conventional cylindrical optic, such a beam will never have the uniform intensity distribution unless only the middle part of the beam will be used for surface structuring, which clearly wastes laser power and limits the width of created features.

In order to demonstrate the capability of the 36DM1 device for the generation of a flat-top stripe, the final spherical lens (f_6) before the CCD camera (see Fig. 7) was replaced by a 200 mm FL cylindrical lens. In addition, the deformable mirror was rotated by 90°, so that the stripe beam was displayed horizontally on the CCD array, i.e., in the direction where more pixels of the array were available. In such a configuration, a Gaussian-distributed stripe was easily produced when the flat reference mirror was placed instead of 36DM1, as can be seen in Fig. 10. The beam captured by the CCD camera was approximately 1.4 mm wide and 0.1 mm tall (measured at the full width at half maxima – FWHM).

The flat-top stripe was generated with the use of the SA algorithm. The target beam was a 300 × 10 pixel rectangle. This should correspond to a 2.22 × 0.074 mm flat-top beam on the CCD array. The initial value of actuator voltages was 90 V. The SA optimization was run for 2000 iterations with the *algorithm temperature* of 0.9 and the *change factor* of 40. The best shape shaping results for these settings are shown in Fig. 11.

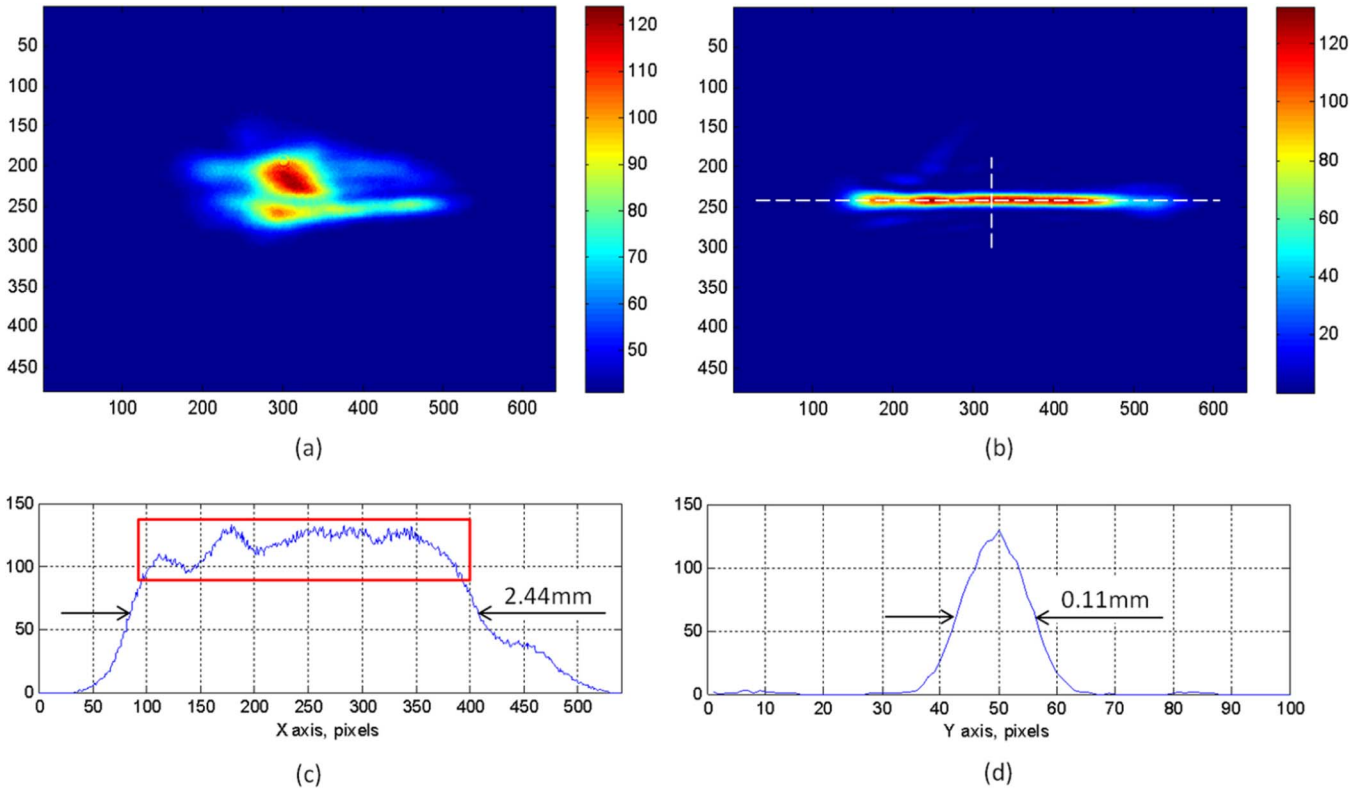

FIG. 11. Flat-top stripe generated by the 36DM1 device: (a) initial shape of the beam before the SA optimization, (b) the best shaping result, (c) horizontal, and (d) vertical profile of the shaped beam.

Figure 11 shows (a) the initial beam before the SA optimization, (b) the best shaping results, and (c) and (d) the cross-sections of the shaped beam which were taken along the dashed lines shown in (b). The shaped stripe was measured to be 2.44 mm wide and 0.11 mm tall, and thus the dimension was very similar to the target design. The flat region of the shaped beam – see the box in Fig. 11(c) – was spread over a 2.1 mm distance, proving the successful operation of the 36DM1 device.

Finally, it has to be noted that we have not yet tested the SA-PDM-shaped flat-top stripe in the *YAGboss* process, because it requires a wavelength of 343 nm, which is beyond the range of operation of the 36DM1 device (HR coating for 1064 nm).[5] However, our plan is to apply a 343 nm HR-coating in the next version of SA-PDM.

IV. CONCLUSIONS AND FUTURE WORK

In this paper, we evaluated the performance of a potentially low cost and scalable SA-PDM. A key aim of our project was to reduce the manufacturing cost of SA-PDMs, so that these attractive devices can be more widely used by the industry and scientists. The regular arrangement of actuators in the 36DM1 device opens the opportunity to scale-up the deformable mirror. Currently, we are developing a 20 mm square aperture SA-PDM, which will have 14 × 14 (196) actuators, i.e., the same mirror size as 36DM1 but the pitch between actuators will be reduced to only 1.27 mm. Our plan is to apply this DM in new generation telescopes and in industrially focused research.

The proof of concept experiments presented in this paper showed that our DM can be successfully used to shape a high power laser beam for laser machining applications. By applying an extension sensing technique and reducing the initial curvature of the mirror surface, it is very likely that we will generate a DM that can be run in the open loop, so that it can be used for "on-the-fly" laser machining, i.e., by using two sets of pre-determined actuator voltages it will be possible to switch between the beam shapes during the machining processes.

ACKNOWLEDGMENTS

The work presented here was supported by several bodies: the Engineering and Physical Sciences Research Council (U.K.) (Grant No. EP/F02553X/1), the Science and Technology Facilities Council (STFC), the Scottish University Physics Alliance (SUPA), the Institute for Integrated Systems (a part of the Edinburgh Research Partnership), and Renishaw plc (UK). We also acknowledge Teer Coatings Ltd (UK) for the help in the development of the process of forming side electrodes in piezoceramic planks.

[1]C. Nusser, I. Wehmann, and E. Willenborg, "Influence of intensity distribution and pulse duration on laser micro polishing," Phys. Proc. **12A**, 462–471 (2011).
[2]R. J. Beck, J. P. Parry, J. D. Shephard, and D. P. Hand, "Adaptive extracavity beam shaping for application in nanosecond laser micromachining," Proc. SPIE **7913**, 79130D (2011).
[3]L. Migliore, "Enhancing silicon cutting performance by shaping the focused beam," Proc. SPIE **6458**, 64580W (2007).
[4]J. M. Bovatsek and R. S. Patel, "Highest-speed dicing of thin silicon wafers with nanosecond-pulse 355 nm q-switched laser source using line-focus fluence optimization technique," Proc. SPIE **7585**, 75850K (2010).
[5]N. J. Weston, D. P. Hand, S. Giet, and M. Ardron, "A method of forming an optical device," patent application WO/2012/038707 (29 March 2012).
[6]J. W. Hardy, J. E. Lefebvre, and C. Koliopoulos, "Real-time atmospheric compensation," J. Opt. Soc. Am. **67**, 360–369 (1977).
[7]F. Roddier, *Adaptive Optics in Astronomy* (Cambridge University Press, 1999).
[8]A. Greenaway, "Adaptive optics technologies for industrial, medical applications," in *Proceedings of the Conference on Lasers and Electro-Optics/Quantum Electronics and Laser Science and Photonic Applications Systems Technologies* (Optical Society of America, 2005), Paper CThE1.
[9]P. Y. Madec, "Overview of deformable mirror technologies for adaptive optics and astronomy," in *SPIE Astronomical Telescopes + Instrumentation* (International Society for Optics and Photonics, 2012), pp. 844705–844718.
[10]M. Loktev, O. Soloviev, and G. Vdovin, *Adaptive Optics Guide* (OKO Technologies, 2008), see http://www.okotech.com/catalogue.
[11]G. Vdovin, M. Loktev, and A. Simonov, "Low-cost deformable mirrors: Technologies and goals," Proc. SPIE **5894**, 58940B (2005).
[12]I. Elder, D. Legge, and J. Beedell, "End-pumped Q-switched Nd:YVO4 laser," Proc. SPIE **6397**, 639705 (2006).
[13]R. J. Beck, J. P. Parry, W. N. MacPherson, A. Waddie, N. J. Weston, J. D. Shephard, and D. P. Hand, "Application of cooled spatial light modulator for high power nanosecond laser micromachining," Opt. Express **18**, 17059–17065 (2010).
[14]L. Golan and S. Shoham, "Speckle elimination using shift-averaging in high-rate holographic projection," Opt. Express **17**, 1330–1339 (2009).
[15]J. P. Parry, R. J. Beck, J. D. Shephard, and D. P. Hand, "Application of a liquid crystal spatial light modulator to laser marking," Appl. Opt. **50**, 1779–1785 (2011).
[16]S. A. Henck, "Lubrication of digital micromirrordevices™," Tribol. Lett. **3**, 239–247 (1997).
[17]H. Liu and B. Bhushan, "Nanotribological characterization of digital micromirror devices using an atomic force microscope," Ultramicroscopy **100**, 391–412 (2004).
[18]B. Bhushan and H. Liu, "Characterization of nanomechanical and nanotribological properties of digital micromirror devices," Nanotechnology **15**, 1785 (2004).
[19]D. Dudley, W. M. Duncan, and J. Slaughter, "Emerging digital micromirror device (DMD) applications," Proc. SPIE **4985**, 14–25 (2003).
[20]Z. Kuang, W. Perrie, D. Liu, S. Edwardson, J. Cheng, G. Dearden, and K. Watkins, "Diffractive multi-beam surface micro-processing using ps laser pulses," Appl. Surf. Sci. **255**, 9040–9044 (2009).
[21]E. T. Ritschdorff and J. B. Shear, "Multiphoton lithography using a high-repetition rate microchip laser," Anal. Chem. **82**, 8733–8737 (2010).
[22]A. Piqué, R. C. Y. Auyeung, A. T. Smith, H. Kim, S. A. Mathews, N. A. Charipar, and M. A. Kirleis, "Laser transfer of reconfigurable patterns with a spatial light modulator," Proc. SPIE **8608**, 86080K (2013).
[23]R. C. Y. Auyeung, H. Kim, N. A. Charipar, A. J. Birnbaum, S. A. Mathews, and A. Piqué, "Laser forward transfer based on a spatial light modulator," Appl. Phys. A **102**, 21–26 (2011).
[24]T. G. Bifano, J. Perreault, R. Krishnamoorthy Mali, and M. N. Horenstein, "Microelectromechanical deformable mirrors," IEEE J. Sel. Top. Quant. **5**, 83–89 (1999).
[25]T. Bifano, "Adaptive imaging: MEMS deformable mirrors," Nat. Photonics **5**, 21–23 (2011).
[26]I. Hook, *Equipping the European Extremely Large Telescope* (SPIE Newsroom, 2012), see http://spie.org/x87013.xml?ArticleID=x87013.
[27]M. Strachan, R. Myers, K. Cooke, J. Hampshire, J. Hough, S. Rowan, M. van Veggel, K. Kirk, D. Hutson, E. Uzgur, and S. S. Kim, "Novel technologies for small deformable mirrors," Proc. SPIE **7736**, 773661 (2010).
[28]E. Uzgur, S. S. Kim, E. Bryce, D. Hutson, M. Strachan, and K. J. Kirk, "Extension sensing of piezo actuators using time-domain ultrasonic measurement and frequency-domain impedance measurement," J. Electroceram. **27**, 38–44 (2011).

[29]E. Bryce, E. Uzgur, D. Hutson, K. Kirk, M. Strachan, N. Schwartz, and P. Parr-Burman, "Overcoming hysteresis in multilayered piezoceramic actuators used in adaptive optics," Proc. SPIE **8342**, 83420O (2012).
[30]D. Bertsimas and J. Tsitsiklis, "Simulated annealing," Stat. Sci. **8**, 10–15 (1993).
[31]S. Campbell, S. Triphan, R. El-Agmy, A. Greenaway, and D. Reid, "Direct optimization of femtosecond laser ablation using adaptive wavefront shaping," J. Opt. A: Pure Appl. Opt. **9**, 1100–1104 (2007).
[32]R. El-Agmy, H. Bulte, A. Greenaway, and D. Reid, "Adaptive beam profile control using a simulated annealing algorithm," Opt. Express **13**, 6085–6091 (2005).